VISCOELASTICITY OF DENTAL HARD TISSUES

S. M. Dub,[a] **K. E. Pechkovs'kyi,**[b,1] **I. M. Pechkovs'ka,**[c]
and M. L. Trunov[d,e]

UDC 539.533:616.314

The results of a study of the mechanical properties of dental hard tissues by nanoindentation are presented. With quasi-static nanoindentation, the analysis of the Berkovich indenter unloading curve allowed to determine the hardness and modulus of elasticity of dental enamel, dentin, and photopolymer composite, which is used for splinting and filling. The hardness and modulus of elasticity of dental enamel was shown to approach that of glass. The hardness and modulus of elasticity of dentin is noticeably lower than that of enamel. The tests revealed the viscoelastic mechanical behavior of enamel, dentin, and photopolymer composite fillings. To determine the viscoelastic characteristics of dental hard tissues, nanoindentation with pulsed load application to the indenter with tracking the change in the depth of impression as a result of viscoelastic deformation relaxation in the nanocontact after the rapid unloading of the indenter was used. For the first time, relaxation times for enamel and dentin have been determined. Rapid indenter unloading made it possible to separate the deformation components (elastic, viscoelastic and plastic) in the nanocontact for these materials. While the proportion of viscoelastic deformation in the total deformation for dental enamel is insignificant (about 2%), for dentin and photopolymer fillings it is significantly higher (~10%). The results indicate that increasing the content of organic components in biomaterials reduces their hardness and modulus of elasticity and increases their viscoelasticity.

Keywords: dental hard tissues, nanoindentation, hardness, modulus of elasticity, viscoelasticity.

Introduction. Information about the mechanical properties of dental hard tissues is essential for improving the quality of restorative dentistry. Ideally, the filling material should not only form a strong chemical bond with dental hard tissues, but also have mechanical properties similar to those of enamel and dentin. For example, a significant difference between the moduli of elasticity of the filling and enamel leads to a different value of deformation, which occurs when chewing solid food, and the concentration of stresses at the filling enamel interface. As a result, microcracks can form at the interface, which will contribute to the occurrence of secondary or restored caries. Therefore, it is important to determine the mechanical characteristics of dental hard tissues and filling materials. Now there are a number of publications dealing with the study of the mechanical properties of dental hard tissues by tensile, bending and torsion tests [1, 2]. But the usual methods of mechanical testing in this case are of little use because of the small sample size and the heterogeneity of dental hard tissues (enamel and dentin). Local methods of mechanical testing, such as hardness testing, are more suitable for testing heterogeneous biological objects [3, 4].

[a]Bakul Institute for Superhard Materials, National Academy of Sciences of Ukraine, Kyiv, Ukraine. [b]Bogomolets National Medical University, Kyiv, Ukraine ([1]konpech@i.ua). [c]Private Higher Educational Institution "Kyiv Medical University", Kyiv, Ukraine. [d]Institute of Information Registration Problems, National Academy of Sciences of Ukraine, Kyiv, Ukraine. [e]Uzhhorod National University, Uzhhorod, Ukraine. Translated from Problemy Prochnosti, No. 6, pp. 107 – 116, November – December, 2021. Original article submitted November 24, 2020.
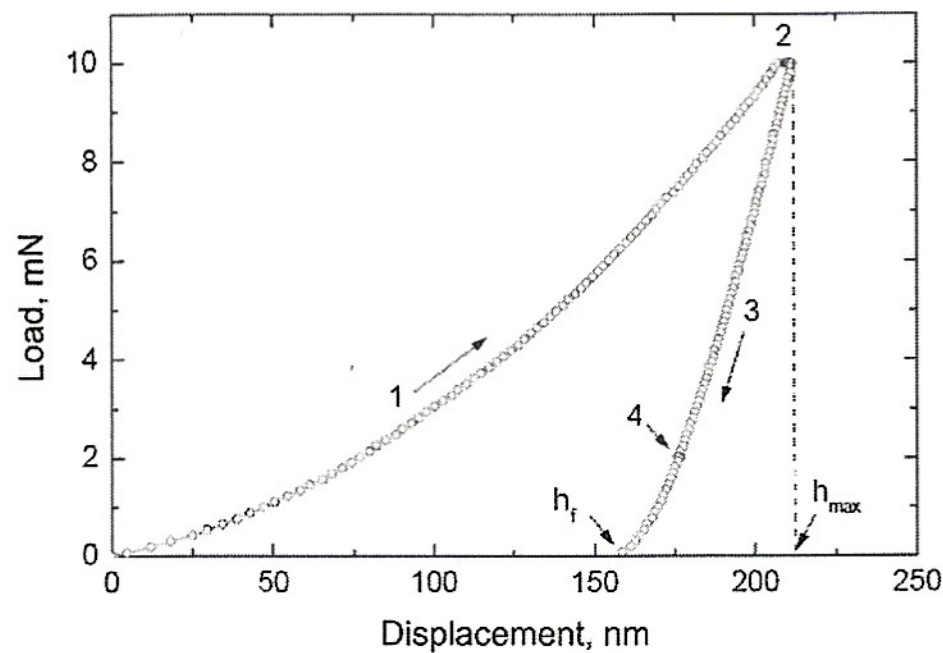
Fig. 1. Berkovich indenter loading curve obtained for a sample of hardened steel: (*1*) indenter load increase portion; (*2*) keeping the indenter under maximum load; (*3*) indenter unloading; (*4*) unloading stop to measure thermal drift in the device.

In hardness tests, a pyramidal diamond indenter is pressed into the flat polished surface of the specimen. As a result, a plastic indentation is formed on its surface, the dimensions of which characterize the resistance of the material to plastic deformation. For indentations from pyramidal indenters (Vickers, Knoop, Berkovich), the law of similarity is fulfilled. Therefore, indentation must occur at a constant ratio of load to indentation area. This ratio is commonly referred to as hardness. Hardness testing is a universal method of mechanical testing, which covers an almost unlimited range of solids from the softest to the hardest. Important advantages of the method are its high locality and simple specimen requirements. A flat polished surface of a few square mm is sufficient for hardness testing. The main disadvantage of the traditional hardness testing method is that the dimensions of the indentation are measured after the test and no information about the mechanical behavior of the specimen is recorded during the test.

In the mid 60's of the last century another method of hardness testing began to develop – indentation depth hardness testing. Significant contribution to the development of this method was made by M. H. Shorshorov, V. P. Alekhin, S. I. Bulychev et al. at the Baikov Institute of Metallurgy of the USSR Academy of Science [5, 6]. During such tests, the displacement of a diamond indenter is recorded both during an increase in load and during unloading. As a result, an indentation diagram is obtained (Fig. 1), which can be used to determine the hardness from the indentation depth. This approach eliminates the need for the laborious and often unreliable measurement of indentation dimensions at low indenter loads. Because the indenter unloading process is elastic, it is possible to estimate the modulus of elasticity of the sample.

The method of measuring hardness based on indentation depth was further developed in the works of Pethicai, Hutchings, and Oliver [7]. By increasing the accuracy of indenter displacement measurement to 0.1 nm (10^{-10} m), they made a breakthrough in 1983 in the region of indentation depths much less than 1 micron. In 1992, Oliver and Pharr developed a method for determining hardness and the modulus of elasticity from the indentation depth under maximum load [8], which is generally accepted. Today, there are a large number of publications devoted to the study of the mechanical properties of dental hard tissues by nanoindentation [4, 9, 10]. Nanoindentation is also used to study the effect of dental hard tissue diseases on the mechanical properties of enamel and dentin [11]. However, in all these works, only the hardness H and the elastic modulus E of dental hard tissues were determined. However, biomaterials are characterized by viscoelasticity, so conventional quasi-static nanoindentation in this case does not provide complete information about their mechanical properties [12]. To separate the strain components in tests of viscoelastic materials, it is necessary to quickly unload the indenter [13, 14]. Below are the results of studying hardness, elastic modulus, and viscoelastic properties of dental hard tissues by nanoindentation, both conventional (quasi-static) and with impulsive loading of the indenter.
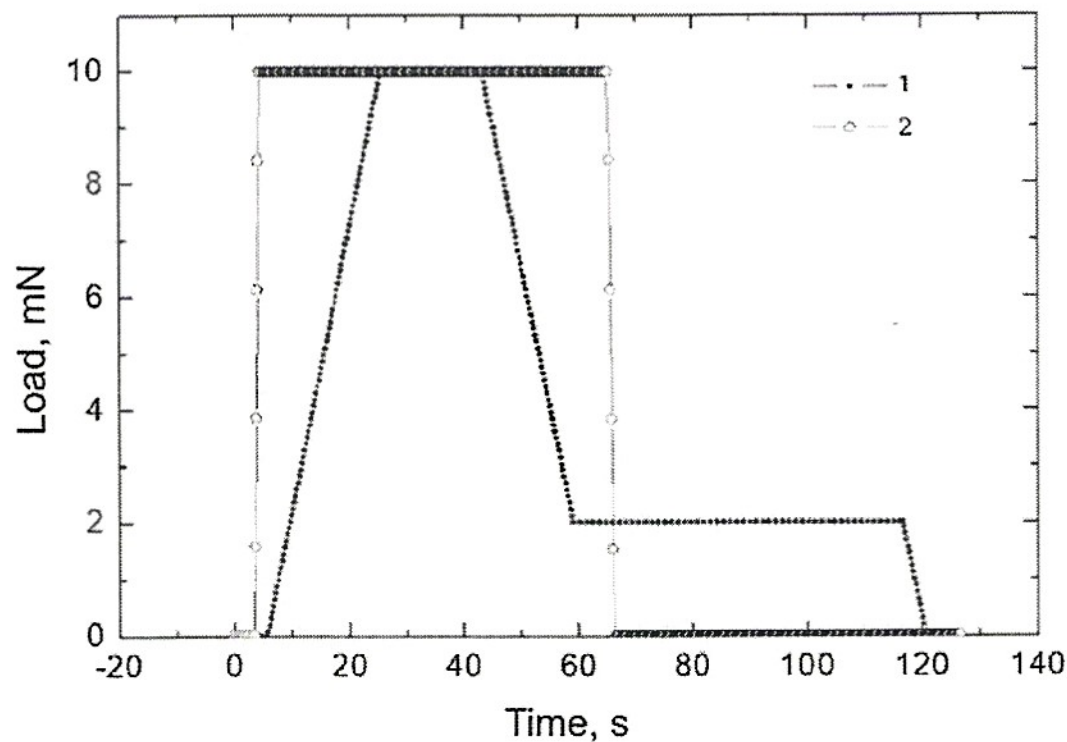
Fig. 2. Dependence of the load on the indenter on time during normal (*1*) and pulsed (*2*) modes of nanoindentation [14].

Experimental Part. A sample of a filled tooth (molar) was cut with a diamond wheel in longitudinal direction into plane parallel plates about 1 mm thick. Then the plates were polished on chamois leather with 3 to 5 μm diamond powder. Final polishing was done with less than 1 micron diamond powder. The tests were carried out on a Nano Indenter II honohardness tester (Nano Instruments, Inc.) with a Berkovich indenter (trihedral pyramid) using two methods. The standard nanohardness test method was used to determine the hardness and modulus of elasticity, the method of impulsive loading of the indenter was used to study the viscoelasticity of dental hard tissues. The maximum load on the indenter was 10 mN (~1 g) for standard tests and 20 mN for impulsive loading. The rate of load increase was 0.5 and 20 mN/s, respectively.

In the standard test scheme (in Fig. 2 line *1*), the load P on the Berkovich indenter linearly increases for 20 s from zero to the maximum P_{max}, is maintained at it for 20 s, and then linearly decreases to the value $P = 0.2P_{max}$. During unloading, a stop is made for 60 s to measure the rate of thermal expansion of the indenter rod. It is assumed that when the latter is held at low load (20% maximum), the change in the depth of indentation is due only to the thermal expansion of the rod through the temperature difference between the sample and the indenter [8]. This allows the thermal expansion rate of the indenter rod to be determined and corrections to measurement results to be made. Then the indenter is completely unloaded. It is recommended that the indenter be unloaded not too quickly (20–30 s) to obtain a sufficient number of measurements to reliably determine the hardness and modulus of elasticity of the sample. The depth of indentation after complete unloading is not monitored and is assumed to be constant. This test scheme is well suited for conventional elastic-plastic materials (metals and ceramics).

However, for viscoelastic materials (e.g., polymers) in which intense relaxation processes occur at room temperature, the standard nanohardness test scheme is unsuitable. Therefore, a scheme with pulsed load application to the indenter was proposed [14]. In such tests, the loading and unloading of the indenter are performed in 1 second, and the depth of indentation is recorded for 60 s after the rapid and complete unloading of the indenter (in Fig. 2, line *2*). Rapid unloading allows the elastic, viscoelastic and plastic components of indenter displacement to be separated and the viscoelastic characteristics to be determined.

The indentations were made on enamel, dentin, and a photopolymer composite (Flow Composite, Oxomat-AN, Ukraine), which is used for dental restorations (Fig. 3). Sapphire, hardened steel (elastic-plastic materials), and PMMA (viscoelastic material) were also tested for comparison. The hardness H and the elastic modulus E were determined using the Oliver and Pharr method by analyzing indenter unloading curves [8]. The viscoelastic properties were determined by the method given in [14].
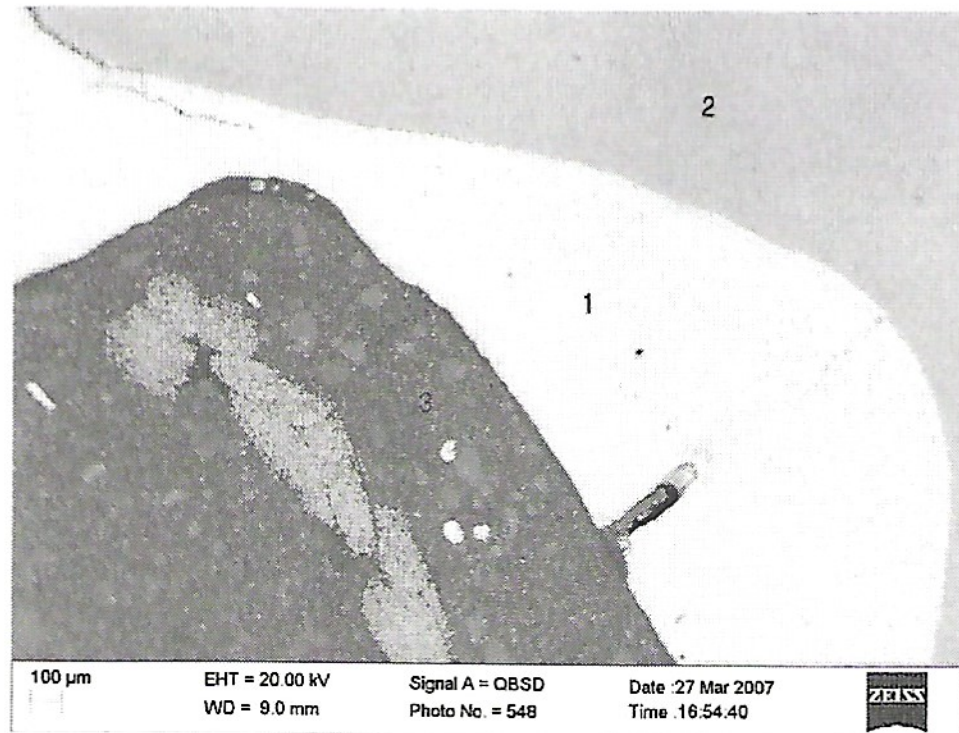
Fig. 3. SEM image of a tooth section perpendicular to the direction of fiber armatures in the area of the longitudinal fissure of the 26th tooth: (*1*) enamel; (*2*) dentin; (*3*) photopolymer composite filling the numerals denote the locations of hardness impressions.
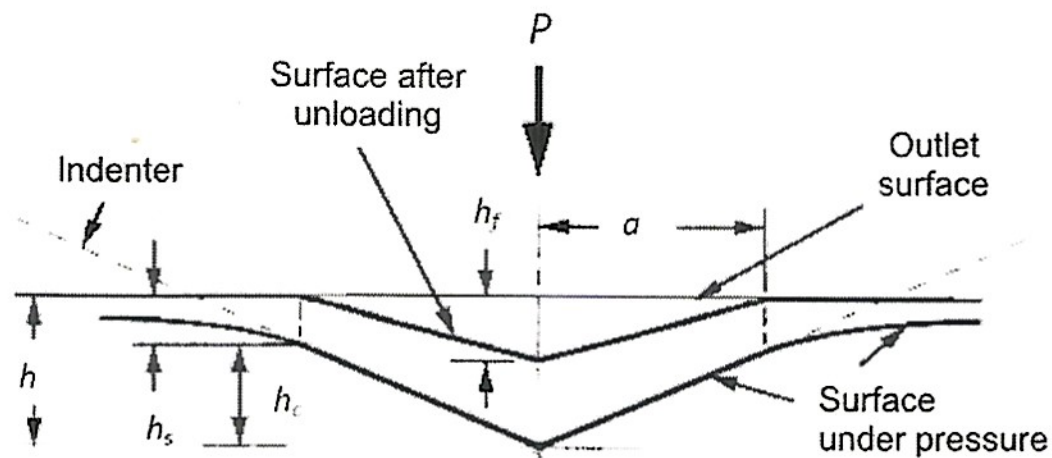

Fig. 4. Change in the shape of indentation when unloading the indenter [8].

Analysis of Nanoindentation Data. The Meyer hardness is the average contact pressure, it is equal to the ratio of load to the projection area of indentation. So, the key of objective the analysis of experimental nanoindentation data is to determine the projection area of the indenter contact with the sample from the depth of indentation at the maximum load without obtaining an image of the indentation. The difficulty lies in the fact that the device measures displacement h, which is equal to the sum of the depth of indentation h_c, and the elastic deflection at its edge h_s (Fig. 4):

$$h = h_s + h_c, \qquad (1)$$

Therefore, to determine the depth of indentation at the maximum load, it is necessary to know the value of the elastic deflection at the edge of indentation. The most common method of analysis is the Oliver and Pharr method [8]. We approximate the unloading curve by a power function in the form of

$$P = B(h_{max} - h_f)^m, \qquad (2)$$

where P is load, mN, h_{max} is displacement at the maximum load, nm, B and m are coefficients, and h_f is indentation imprint depth after full unloading, nm (Figs. 1 and 4).

Using the coefficients B and m, we determine the stiffness S of the initial portion of the indenter unloading curve (Fig. 1):

$$S = \frac{dP}{dh} = mB(h_{max} - h_f)^{m-1},$$ (3)

where S is the contact stiffness, N/m.

The elastic deflection of the surface at the contact edge is determined from the equation [8]

$$h_s = \varepsilon \frac{P_{max}}{S},$$ (4)

where ε is a constant for the Berkovich indenter, $\varepsilon = 0.75$. Hence the depth of indentation at the maximum load will be

$$h_c = h_{max} - \varepsilon \frac{P_{max}}{S}.$$ (5)

For a perfectly sharp Berkovich indenter, the projection area of indentation, A_c is

$$A_c = 24.56 h_c^2.$$ (6)

But a real Berkovich indenter always has at the apex a bluntness, the shape of which is close to spherical. The bluntness radius cannot be made smaller than 50 nm. It gradually increases to 100–200 nm when operating the nanohardness meter. The equation (6), which relates the height of the trihedral pyramid, h, to the base area A, can only be used at relatively large depths, at which bluntness at the indenter tip can be neglected. At shallow depths, the contact area calculated from formula (6) will differ from the real area. The shallower the contact depth, the larger the error will be. To account for the effect of blunting, the indenter shape function is used in the form of

$$A_c = 24.56 h^2 + C_1 h^1 + C_2 h^{1/2} + C_3 h^{1/4} + ... + C_8 h^{1/128},$$ (7)

where $C_1, ..., C_8$ are constants, which are used to find the projection area of indentation at shallow depths [7].

Due to the automatic calibration of the device, these constants are selected so that the elastic modulus of a standard sample of fused quartz (supplied with the device) does not depend on the depth of contact and is 72 GPa.

Knowing the contact projection area A_c, we can determine the hardness H and the reduced modulus of elasticity E_r:

$$H = \frac{P_{max}}{A_c},$$ (8)

$$E_r = \frac{\sqrt{\pi S}}{2\beta \sqrt{A_c}}.$$ (9)

So, the Oliver and Pharr method allows us to determine the contact projection area, hardness and modulus of elasticity of the sample without obtaining an image of indentation.

Results of the Study and Their Discussion. A typical Berkovich indenter loading curve for standard nanohardness tests for a hardened steel specimen is shown in Fig. 1. As the indenter load increases to 10 mN, the depth of the indentation increases to 208 nm. When the indenter was kept under maximum load for 20 s, the depth increased by another 3 nm due to creep in the contact, while during unloading it decreased to 158 nm as a result of the relaxation of elastic stresses in the contact area. Most materials have similar indentation diagrams, which differ only in the depth of indentation at the maximum load (determined by the hardness of the material) and the amount of
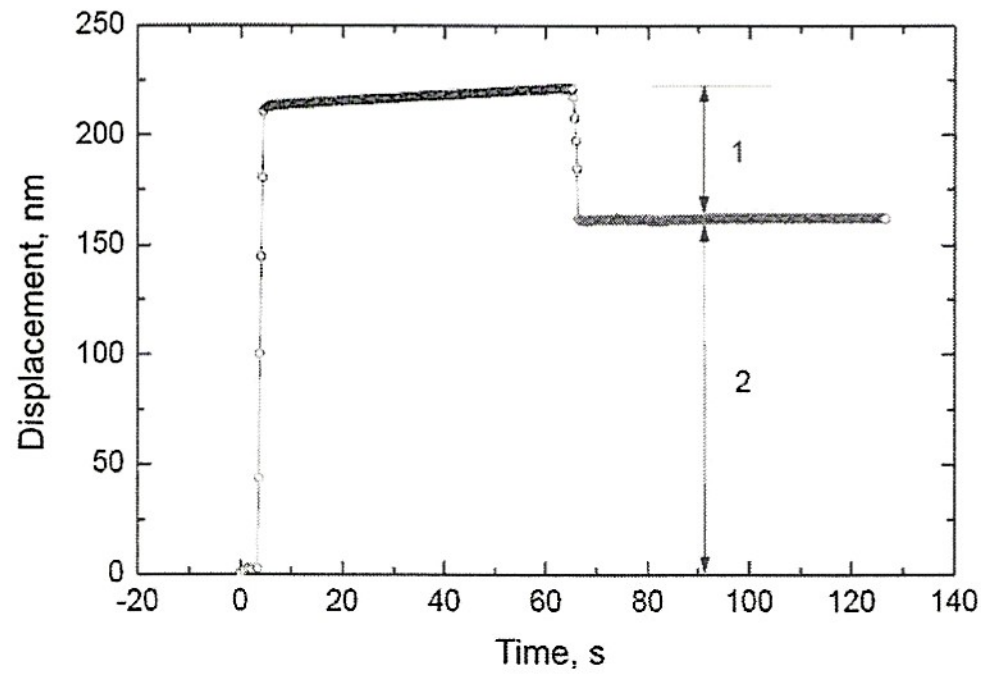
Fig. 5. Time dependence of indenter displacement for an elastic-plastic material (steel) under impulsive loading: (*1*) elastic component of indenter displacement (elastic recovery under unloading); (*2*) plastic component.
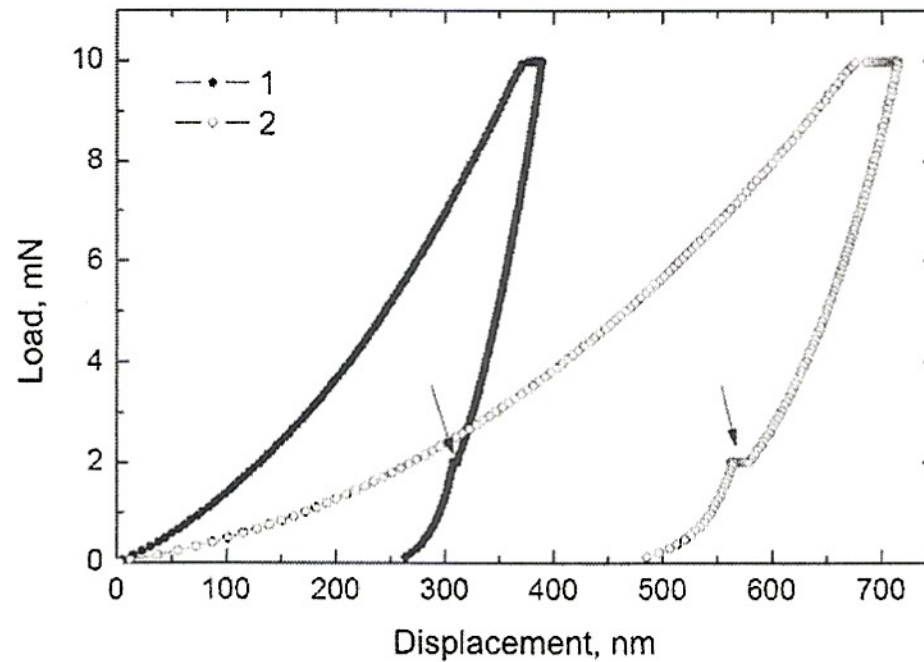

Fig. 6. Berkovich indenter loading curves for dental enamel (*1*) and dentin (*2*). (The arrows show the steps, which were formed through the relaxation of viscoelastic deformation during the stop of indenter unloading to measure the thermal drift in the device.)

elastic recovery (determined by the ratio of hardness to the modulus of elasticity). The time dependence of the depth of indenter penetration into steel under impulsive loading is shown in Fig. 5. It can be seen that the depth of indentation after rapid unloading does not change for steel. This indicates that not only elastic but also plastic deformation took place when the indenter penetrated the steel. This mechanical behavior (Figs. 1 and 5) is characteristic of metals and ceramics, which are elastic-plastic materials.

Typical Berkovich indentation diagrams for dental hard tissues are shown in Fig. 6. It can be seen that under the same load, the depth of the indentation in enamel is much less than in dentin, which is indicative of its higher hardness. The unloading curves for dental enamel, and especially for dentin and photopolymer fillings, show steps at the moment of stopping unloading to measure the thermal drift rate in the device. Such steps are not present in normal elastic-plastic materials (Fig. 1). But their formation is characteristic of viscoelastic materials, particularly polymers [15, 16]. This is due to the time dependence of their mechanical properties. If these materials are quickly unloaded, the depth of indentation will change for some time after unloading (Fig. 7) due to viscoelastic deformation
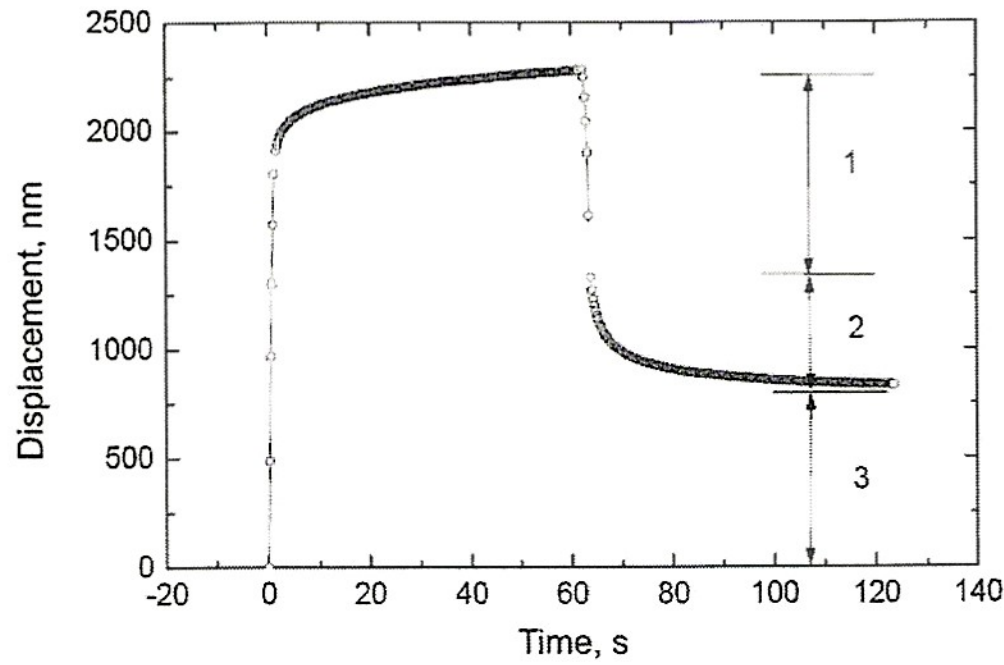
Fig. 7. Time dependence of indenter displacement for a viscoelastic material (PMMA polymer) under impulsive loading: (*1, 2, 3*) elastic, viscoelastic, and plastic components of indenter displacement, respectively.
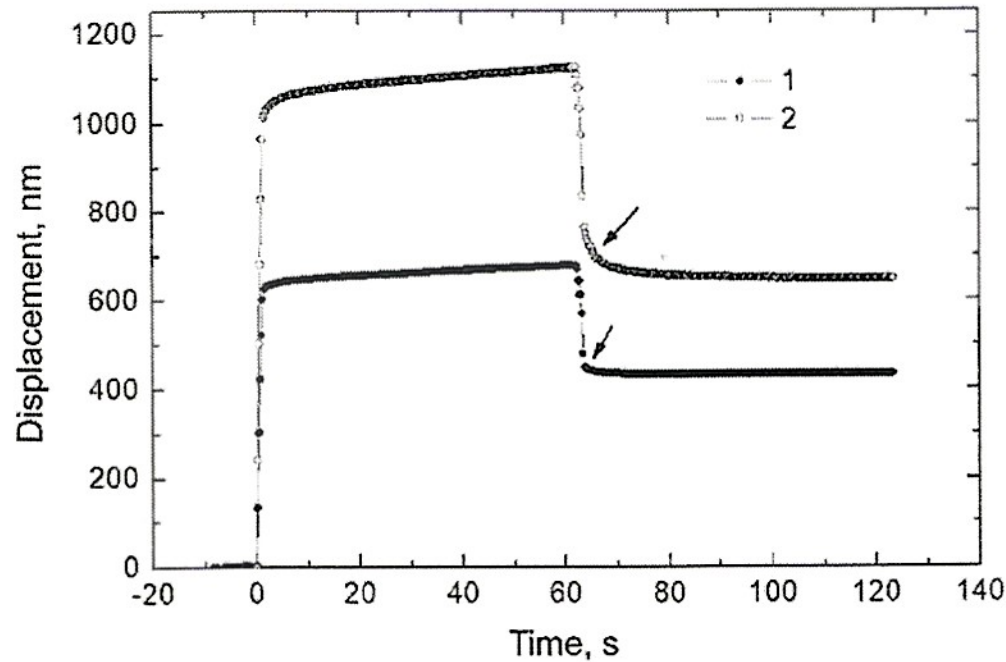

Fig. 8. Time dependence of indenter displacement for dental hard tissues: (*1*) enamel; (*2*) dentin. (The arrows indicate viscoelastic relaxation in indentation.)

relaxation in the contact area. Therefore, during the unloading stop to measure thermal drift, the indenter displacement changes not only through thermal drift, but also through the viscoelastic recovery of indentation. So, the formation of steps on the unloading curve (Fig. 6) suggests that dental hard tissues are viscoelastic materials. To verify this assumption, we tested dental hard tissues by the impulsive loading of the indenter and tracking the change in the depth of indentation after its complete unloading. Figure 8 shows that the depth of impression continues to decrease after full unloading, which confirms the assumption of viscoelasticity of dental enamel and dentin. The time dependence of the indentation depth h after the full unloading of the indenter is described by the equation:

$$h = h_0 + h_{rel\,max}\,e^{-t/\tau},$$ (10)

where h_0 is the minimum depth to which the indentation relaxes (in this case, $h_0 = h_{plast}$), nm, $h_{rel\,max}$ is the maximum value of indentation relaxation recovery (Fig. 9), nm, and τ is the indentation relaxation time. This is the time during which the depth of indentation decreases by a factor of e (Euler number e is equal to ≈ 2.718).

924

TABLE 1. Hardness H and modulus of elasticity E of Dental Hard Tissues and Photopolymer Composite Fillings. Quasi-Static Nanoindentation, Load 10 mN

Material	Depth of indentation, nm	E, GPa	H, GPa
Sapphire[1]	120 ± 3	395 ± 15	29.0 ± 0.5
Steel[2]	212 ± 6	225 ± 3	9.3 ± 0.5
Glass[3]	335 ± 8	60 ± 2	5.1 ± 0.3
Tooth enamel	410 ± 18	63 ± 5	2.9 ± 0.2
Dentin	676 ± 33	27 ± 2	1.2 ± 0.1
Copper[4]	811 ± 24	129 ± 5	0.65 ± 0.05
Filling[5]	1323 ± 17	9 ± 1	0.4 ± 0.1
PMMA[6]	1455 ± 17	4.5 ± 0.1	0.30 ± 0.01

Notes. 1. Monocrystal, basal plane. 2. Hardened steel, hardness standard for Matsuzawa MXT70 microhardness tester. 3. Flint grade TF-5. 4. Plane (111) of copper monocrystal. 5. Oxomat-AN polymer-based composite. 6. Polymethylmethacrylate.
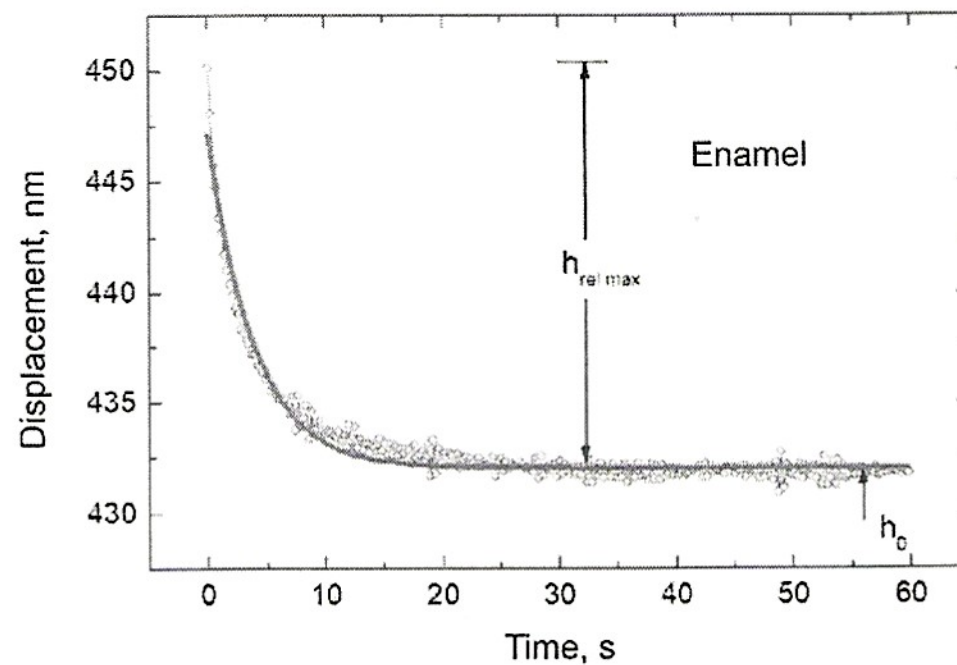

Fig. 9. Curve of the viscoelastic recovery of indentation in dental enamel and the result of its approximation by exponential function.

The results of the determination of hardness and modulus of elasticity by the method of Oliver and Pharr are shown in Table 1. It can be seen that the hardness of enamel is approximately 2.9 GPa. This is almost four times higher than the hardness of copper (0.65 GPa), but much lower than the hardness of sapphire (29 GPa), the second natural material in hardness after diamond. The hardness of enamel is the upper limit of hardness for biobjects. It seems that there are no harder biobjects in nature, at least in humans. The hardness of dentin is noticeably lower than that of enamel, approximately 1.2 GPa. The higher hardness of enamel compared to dentin is probably due to the higher degree of mineralization (96 and 70%, respectively). The low modulus of elasticity of enamel and especially dentin indicates that biomaterials deform elastically relatively easily compared to metals. For hardness and modulus of elasticity, dental enamel is close to glass (Table 1). The H and E values obtained correspond to the data given in the literature [4, 9, 11].

The results of impulsive loading tests are shown in Table 2. The relaxation time for enamel and dentin is half as long as for polymethyl methacrylate and photopolymer fillings and is approximately 4 s. But the viscoelastic component of indenter displacement for dentin is much higher than for enamel. So, the viscoelastic mechanical behavior of dentin is much more pronounced than that of enamel. This indicates that an increase in the proportion of

TABLE 2. Proportion of Elastic, Viscoelastic, and Plastic Displacement (%) in the Total Displacement of the Indenter and the Time of Viscoelastic Relaxation

Material	Displacement			h_0, nm	$h_{rel\ max}$, nm	τ, s
	Elastic	Viscoelastic	Plastic			
Steel	27	0	73	158	0	0
PMMA	42	22	36	849	350	7.9
Enamel	34	2	64	432	15	3.8
Dentin	32	10	58	650	92	4.2
Filling	61	11	27	455	131	9.9

organics in the structure of dental hard tissues leads not only to a decrease in hardness and elastic modulus (Table 1), but also to an increase in their viscoelasticity.

Conclusions. Nanohardness tests of dental hard tissues by standard method and with pulsed load application have been carried out. The hardness and modulus of elasticity of enamel, dentin and the material of a photopolymer composite filling have been determined. The viscoelasticity of dental hard tissues has been investigated for the first time. The higher hardness and modulus of elasticity of dental enamel and lower viscoelasticity compared to the same characteristics of dentin are probably due to the higher mineralization of enamel.

REFERENCES

1. F. Eltit, V. Ebacher, and R. Wang, "Inelastic deformation and microcracking process in human dentin," *J. Struct. Biol.*, **183**, No. 2, 141–148 (2013), https://doi.org/10.1016/j.jsb.2013.04.002.

2. D. Zaytsev and P. Panfilov, "Deformation behaviour of human enamel under diametral compression," *Mater. Lett.*, **136**, 130–132 (2014), https://doi.org/10.1016/j.matlet.2014.07.189.

3. J. M. Mattice, A. G. Lau, M. L. Oyen, and R. W. Kent, "Spherical indentation load relaxation of soft biological tissues," *J. Mater. Res.*, **21**, No. 8, 2003–2010 (2006), https://doi.org/10.1557/jmr.2006.0243.

4. L. Angker and M. V. Swain, "Nanoindentation: application to dental hard tissue investigations,, *J. Mater. Res.*, **21**, No. 8, 1893–1905 (2006), https://doi.org/10.1557/jmr.2006.0257.

5. S. I. Bulychev and V. P. Alekhin, *Testing of Materials by Continuous Indentation* [in Russian], Mashinostroenie, Moscow (1990).

6. Yu. I. Golovin, *Nanoindentation* [in Russian], Mashinostroenie, Moscow (2009).

7. J. B. Pethicai, R. Hutchings, and W. C. Oliver, "Hardness measurement at penetration depths as small as 20 nm," *Phil. Mag. A*, **48**, No. 4, 593–603 (1983), https://doi.org/10.1080/01418618308234914.

8. W. C. Oliver and G. M. Pharr, "An improved technique for determining hardness and elastic modulus using load and displacement sensing indentation experiments," *J. Mater. Res.*, **7**, 1564–1583 (1992), https://doi.org/10.1557/JMR.1992.1564.

9. M. S. Zafar and N. Ahmed, "Nano-mechanical evaluation of dental hard tissues using indentation technique," *World Appl. Sci. J.*, **28**, No. 10, 1393–1399 (2013), https://doi.org/10.5829/idosi.wasj.2013.28. 10.1805.

10. Y. L. Chan, A. H. W. Ngan, and N. M. King, "Nano-scale structure and mechanical properties of the human dentine–enamel junction," *J. Mech. Behav. Biomed. Mater.*, **4**, 785–795 (2011), https://doi.org/10.1016/j.jmbbm.2010.09.003.

11. L.-H. He and M. V. Swain, *Nanoindentation of Tooth Tissues*, in: M. L. Oyen (Ed.), *Handbook of Nanoindentation with Biological Applications*, Pan Stanford Publishing, Singapore (2010), pp. 239–277.

12. J. Menčík, L. H. He, and J. Němeček, "Characterization of viscoelastic-plastic properties of solid polymers by instrumented indentation," *Polym. Test.*, **30**, 101–109 (2011), https://doi.org/10.1016/j.polymertesting. 2010.11.006.

13. S. Yang, Y. W. Zhang, and K. Zeng, "Analysis of nanoindentation creep for polymeric materials," *J. Appl. Phys.*, **95**, No. 7, 3655–3666 (2004), https://doi.org/10.1063/1.1651341.

14. S. N. Dub and M. L. Trunov, "Determination of viscoelastic material parameters by step-loading nanoindentation," *J. Phys. D: Appl. Phys.*, **41**, 074024 (2008), http://dx.doi.org/10.1088/ 0022-3727/ 41/7/074024.

15. K. I. Schiffmann, "Nanoindentation creep and stress relaxation tests of polycarbonate: analysis of viscoelastic properties by different rheological models," *Int. J. Mater. Res.*, **97**, 1199–1211 (2006), https://doi.org/ 10.3139/146.101357.

16. A. Dzwilewski, A. Talyzin, G. Bromiley, et al., "Characterization of phases synthesized close to the boundary of C60 collapse at high temperature high pressure condition," *Diam. Relat. Mater.*, **16**, 1550–1556 (2007), https://doi.org/10.1016/j.diamond.2006.12.040.